Bypassing Dynamical Freezing in Artificial Kagome Ice

V. Schánilec, Benjamin Canals, V. Uhlíř, L. Flajšman, J. Sadílek, T. Šikola, Nicolas Rougemaille

Bypassing dynamical freezing in artificial kagome ice

V. Schánilec,[1,2] B. Canals,[1] V. Uhlíř,[2] L. Flajšman,[2] J. Sadílek,[2] T. Šikola,[2,3] and N. Rougemaille[1]
[1] *Univ. Grenoble Alpes, CNRS, Grenoble INP, Institut NEEL, 38000 Grenoble, France*
[2] *Central European Institute of Technology, CEITEC BUT, Brno University of Technology, Purkyňova 123, Brno 612 00, Czech Republic*
[3] *Institute of Physical Engineering, Faculty of Mechanical Engineering, Brno University of Technology, Technická 2, Brno, 616 69, Czech Republic*
(Dated: July 13, 2020)

Spin liquids are correlated, disordered states of matter that fluctuate even at low temperatures. Experimentally, the extensive degeneracy characterizing their low-energy manifold is expected to be lifted, for example because of dipolar interactions, leading to an ordered ground state at absolute zero. However, this is not what is usually observed, and many systems, whether they are chemically synthesized or nanofabricated, dynamically freeze before magnetic ordering sets in. In artificial realizations of highly frustrated magnets, ground state configurations, and even low-energy manifolds, thus remain out of reach for practical reasons. Here, we show how dynamical freezing can be bypassed in an artificial kagome ice. We illustrate the efficiency of our method by demonstrating that the *a priori* dynamically inaccessible ordered ground state and fragmented spin liquid configurations can be obtained reproducibly, imaged in real space at room temperature, and studied conveniently. We then identify the mechanism by which dynamical freezing occurs in the dipolar kagome ice.

Introduction.—Two-dimensional arrays of interacting nanomagnets are powerful model systems to explore experimentally disordered states of matter and to tackle problems of statistical mechanics via a lab-on-chip approach [1–3]. This approach allowed the fabrication of artificially-designed classical Ising spin liquids, whose properties can be probed directly in real space using magnetic imaging techniques [4–6]. Artificial spin systems were extensively studied in the past decade, and the topic is now mature enough to utilise technologies derived from nanomagnetism and spintronics to investigate condensed matter concepts inhered from highly frustrated magnetism. For example, collective magnetic phenomena, such as emergent charge crystallization [7–17], magnetic moment fragmentation [9] and Coulomb phase physics [18–21] have been recently evidenced in artificial frustrated spin systems, complementing what can be done with spin ice compounds [22–27].

In that context, the dipolar kagome ice is particularly interesting as it hosts all these exotic, many-body phenomena [7–9, 25, 28, 29]. The thermodynamics of the dipolar kagome ice consists of four temperature regimes [9, 28, 29] [see Fig.1(a)]: a high temperature paramagnet (PM) evolving in a first spin liquid (SL1) as the system starts to correlate, a fragmented Coulombic spin liquid (SL2) at low temperature [25], and a long range ordered (LRO) ground state. The dipolar kagome ice experiences a critical slowing down when approaching the SL1/SL2 phase transition *and* a freezing of the single spin-flip dynamics [30].

This dynamical freezing is an *intrinsic*, model-dependent mechanism, which prevents the configuration space to be probed ergodically. It is thus strikingly different from other *extrinsic*, sample-dependent mechanisms, which lead to an arrested state after the system has been subjected to a field demagnetization protocol or a thermal treatment for example. Extrinsic processes include quenched disorder [31–33] (distribution of switching fields, of coupling strengths, etc) and variability in the nanomagnets' blocking or Curie temperatures (inhomogeneous magnetic anisotropy, distribution of chemical composition in alloys, etc) in thermally-active systems [34–38]. Consequently, even if one could fabricate an ideal, defect-free sample, dynamical freezing would still be an important obstacle for reaching the low-energy physics of the dipolar kagome ice.

Dynamical freezing is not specific to the dipolar kagome ice and is also present, for example, in the square ice [18, 21] and in the dipolar kagome Ising antiferromagnet [13, 16, 17, 39]. The common feature between the dipolar kagome ice and the square ice is that both models become loop models in their low-energy manifolds. Otherwise said, the spin dynamics that further correlates the system at low temperature is a loop dynamics, in which a string of neighboring spins reverses simultaneously [see Fig.1(b)]. The configuration space can then be explored without breaking the charge crystal associated with the SL2 phase of the dipolar kagome

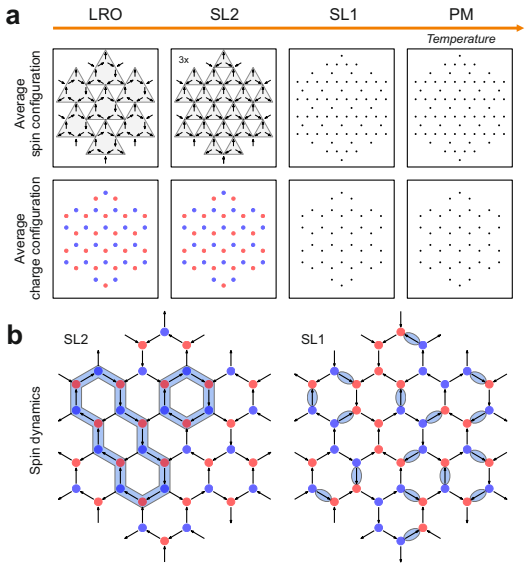

FIG. 1. (a) The top and bottom panels represent the spin and charge states in each of the four phases, averaged over a large number of equilibrated spin configurations. In the top panel, the length of the arrows represents the mean value of the spins after averaging. This length is zero in the PM and SL1 phases, exactly 1/3 in the SL2 manifold and 1 in the LRO ground state. The shaded triangles give the spin unit cell. In the bottom panel, the blue and red dots represent the mean value of the magnetic charges after averaging (blue codes for -1 and red for $+1$). In the PM and SL1 phases, the average charge is zero everywhere, whereas it is ± 1 in the SL2 and LRO phases. (b) Schematics of the spin dynamics involved in the SL1 and SL2 phases. Examples of possible spin flips and loop moves are highlighted in blue.

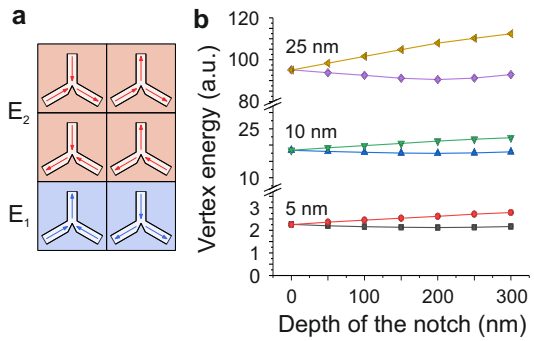

FIG. 2. (a) Schematics illustrating how a notch located at a kagome vertex lifts the sixfold degeneracy between ice-rule states. The two vertices in blue have a lower energy than the four red vertices. (b) Variation of the energy gap $E_2 - E_1$ as a function of the depth of the notch for 5, 10 and 25 nm-thick nanomagnets.

ice, or the divergence-free constraint in the square ice. However, such collective loop moves are unlikely in artificial spin systems and in spin ice compounds, and probing experimentally the low-energy manifolds of these ice models is challenging [40], if ever possible. In the artificial dipolar kagome ice, the LRO state and SL2 phase have never been imaged and studied in real space. Besides, the physical reason why the single spin-flip dynamics freezes remains elusive.

Motivation.— The purpose of this work is twofold. First, we demonstrate experimentally that dynamical freezing can be bypassed in an artificial kagome ice. We are thus able to bring the system, reproducibly and efficiently, into any desired microstate satisfying the ice rule, including the *a priori* inaccessible ordered ground state, but those belonging to the fragmented spin liquid as well. In other words, we show that the system can be set at any desired effective temperature, even absolute zero. Then, we warm up the system to understand how the single spin-flip dynamics acts on those low-energy microstates. Large crystallites of the LRO and SL2 phases are obtained. Imaging the charge domain walls separating neighboring crystallites reveal that *all* spins constituting the walls are unable to flip without breaking the ice rule constraint. Consequently, once the system is at sufficiently low temperature, the charge domain walls are frozen, preventing the charge domains to grow like in conventional spin systems, i.e., by propagating domain walls. Interestingly, this freezing mechanism is also observed for microstates belonging to the SL1 phase, thus unveiling the phenomenon by which the single spin-flip dynamics freezes in the dipolar kagome ice.

Imprinting the desired microstate: The notch rule.—In artificial spin systems, the nanomagnets are usually approximated by Ising pseudo-spins and their micromagnetic nature [41–45] is neglected. Here, micromagnetism is the key ingredient. Our strategy is to imprint a given microstate, vertex by vertex, in a kagome array made of connected nanomagnets, with a notch at each vertex site [see Fig.2(a)]. The idea is to lift, locally, the energy degeneracy between the six states of a given vertex satisfying the ice rule constraint, using micromagnetism as an extra degree of freedom. For magnetostatic reasons, the two configurations in blue in Fig.2(a) have a lower energy E_1 than the four red configurations having an energy E_2. The threefold

symmetry of the vertex is broken and the local low-energy spin state reflects the uniaxial anisotropy induced by the notch. Micromagnetic simulations [46] show that the energy gap $E_2 - E_1$ continuously increases as the depth of the notch is increased, and also increases as the thickness of the nanomagnets increases [see Fig.2(b)]. The notch size is then an external parameter one can play with to force, or statistically ease, the selection of a local spin configuration. It is interesting to note that the notch approach leads to an analogue situation to the vertex type formation in a two-dimensional square lattice [48].

Setting the system temperature.—To test the efficiency of our proposal, we now consider the LRO ground state of the dipolar kagome ice as the target microstate. A series of kagome lattices made of permalloy nanomagnets connected at the vertex sites was fabricated. Our arrays consist of 250 nm-wide, $\sim$1 μm-long and 15 nm-thick nanomagnets. A notch is incorporated at each vertex [see Fig.3(a) and Supp. Fig.1] according to the "notch rule" described above. The depth of the notch ranges typically from 50 to 200 nm, with a top angle of 30°. The kagome lattices, which contain approximately 10^3 nanomagnets, were demagnetized using a field protocol similar to the one used in previous works [7, 18]. The resulting configurations are imaged with a magnetic force microscope [see Figs.3(b-c)].

When the depth of the notch is large (200 nm), the lattices are found in the LRO ground state [see Fig.3(b)]. We emphasize that the LRO ground state is obtained after demagnetizing the lattice using a field protocol. The approach is thus strikingly different from the magnetic writing technique introduced in Ref.49. In particular, the LRO configuration is not restricted to a few spins only, but spans across the entire arrays. The dynamical freezing of the dipolar kagome ice is then efficiently bypassed and the experimentally inaccessible ground state of this model is easily imaged. The same approach works for any microstate of the fragmented spin liquid, i.e., for a disordered spin configuration embedded within a charge crystal [see Supp. Figs.2 and 3.]

Importantly, when the notch size is smaller, or when the demagnetization protocol is made shorter, magnetic disorder appears. In many cases, we imaged an arrested microstate consisting of large crystallites of the LRO or SL2 configuration (depending on the imprinted state), separated by grain boundaries [see Fig.4(a) and Supp. Figs.2 and 3.] In other

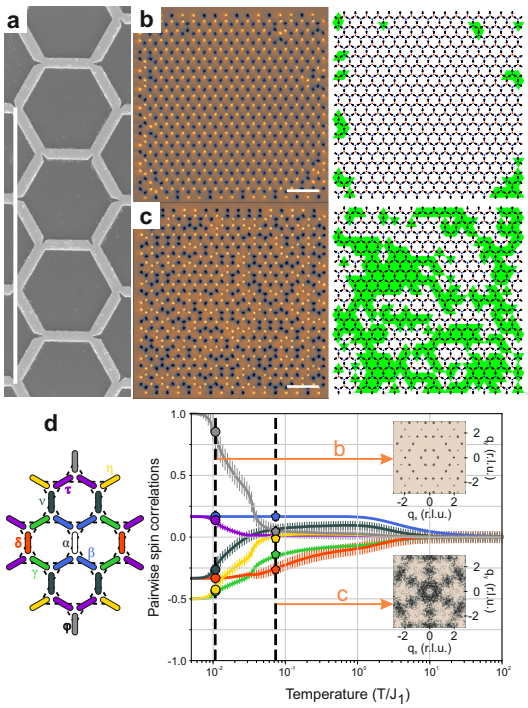

FIG. 3. (a) Electron micrograph of a lattice showing the positions of the notches. (b,c) Magnetic image and resulting spin / charge configuration for a LRO imprinted state and a notch size of 200 nm (b) and 100 nm (c). The two lattices have undergone the exact same demagnetization procedure. In the spin / charge configurations, the spins are represented by black arrows, the vertex charge by a red or blue dot, and the charge domains appear in white or green. 7% (b) and 39% (c) of the vertices break the notch rule. Scale bar is 6 μm. (d) Temperature dependence of the first seven spin-spin correlators. The dots are deduced from the experimental images reported in (b) and (c), illustrating how the effective temperature is affected by the notch size. Insets show the magnetic structure factors associated to the two experimental spin configurations. J_1 is the coupling strength between two nanomagnets not sharing the notch, see Supp. Info.

cases, the spin configurations are more disordered, resembling those of the SL1 phase [see Fig.3(c) and Supp. Fig.2]. Taken as a whole, these results show that the effective temperature of the system can be tuned by a proper choice of the notch parameters and/or demagnetization time. We emphasize that, although we imprint a microstate during the nanofabrication process, this microstate is not frozen, and the thermodynamics of our kagome ice magnet can be probed over an extended (and usually inaccessible) range of effective temperatures. This is illustrated in Fig.3(d) and Supp. Figs.2, where the

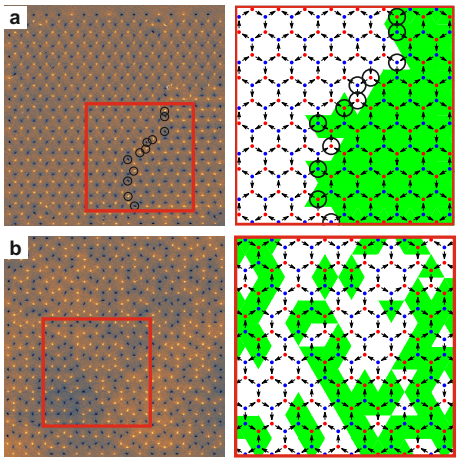

FIG. 4. (a,b) Magnetic image and resulting spin / charge configuration for a LRO imprinted state and a notch size of 200 nm (a), and for a lattice with no notch (b). Color code is the same as in Fig.3. Comparing the two magnetic images reveals the efficiency of the notch strategy. In (a), 4% of the vertices break the notch rule (positions are indicated by a circle).

effective temperature is derived from the comparison between the experimental values of the first seven pairwise spin correlations and those expected in the dipolar kagome ice model [12]. The thermodynamic properties of the spin Hamiltonian describing our experimental system are presented in Supp. Fig.4 [50].

Where does it freeze?— We might then wonder why and where the dipolar kagome ice freezes in the first place. To address this question, we consider the case of charge domains in an LRO microstate [see Fig.4(a)]. These domains are separated by a domain wall. By definition, the spins belonging to a charge domain wall link two vertices carrying the same magnetic charge. Interestingly, flipping these spins is impossible without breaking the ice rule. This is so because they are necessarily minority spins for one of the two vertices they connect (for example, in a "2 in/1 out" vertex configuration, the minority spin is the one pointing "out"). The associated energy cost is then so high that such spin-flip events are unlikely at sufficiently low temperature, specifically in the case we consider here with LRO charge crystallites. The domain wall is thus static, and domain growth cannot occur through the motion of walls.

This freezing mechanism is not restricted to the low-temperature regime, but is also observed in the early stage of the SL1 phase. This is illustrated in Fig.4(b), where a conventional kagome ice (i.e., with no notch) has been demagnetized using the very same field procedure that led to the LRO charge crystallites reported in Fig.4(a). Here as well, the charge domain walls consist of spins that cannot be flipped without breaking the ice rule constraint, regardless of the domain size. This explains why and where the dipolar kagome ice freezes.

As expected for a conventional lattice with no notch, charge domains are very small, and the demagnetization protocol shows strong limitations in reducing the effective temperature of the system. The reason why a notched structure is more efficient to lower the effective temperature than a conventional lattice [see Figs.4(a,b)] is because the notch rule is necessarily broken in a domain wall [see circles in Figs.4(a) and Supp. Fig.3]. Domain walls in a notched structure substantially increase the system energy, making them energetically unfavorable to proliferate. Since the notch size can be chosen at will, this extra energy penalty can be tuned continuously, allowing the investigation of excited states built from the imprinted configuration.

The above arguments explain why exploring the phase diagram of the dipolar kagome ice is challenging experimentally. Contrary to most of the spin systems, the formation of charge domains does not result from a nucleation / propagation process, in which small domains first nucleate and domain walls subsequently extend. Instead, domain growth is solely ensured by the nucleation / annihilation of other domains. Otherwise said, a given charge domain can only grow if the nucleation of other similar domains occur at the same time. Since both charge domains have equal probability to nucleate / annihilate, the system can (very) unlikely approach the SL1 / SL2 transition.

We hope that our experiment, with the associated model, would be useful in engineering of artificial frustrated ice magnets, not only to capture the exotic physics of a given frustrated spin system, but also to reach and manipulate any desired microstate as well. A natural extension of this work would be the implementation of the notch strategy in a thermally-active kagome ice magnet.

This work was supported by the Agence Nationale de la Recherche through project no. ANR-17-CE24-0007-03 'Bio-Ice' and was carried out with the support of the CEITEC Nano Research Infrastructure (MEYS CR, 2016–2019). This work also received funding from the European Union's Hori-

zon 2020 research and innovation under the Marie Skłodowska-Curie program and was co-financed by the South Moravian Region under grant agreement No. 665860.

[1] C. Nisoli, R. Moessner and P. Schiffer, Rev. Mod. Phys. **85**, 1473-1490 (2013).
[2] N. Rougemaille and B. Canals, Eur. Phys. J. B **92**, 62 (2019).
[3] S. H. Skjærvø, C. H. Marrows, R. L. Stamps and L. J. Heyderman, Nat. Rev. Phys. **2**, 13 (2020).
[4] M. Tanaka, E. Saitoh, H. Miyajima, T. Yamaoka and Y. Iye, J. Appl. Phys. **97**, 10J710 (2005).
[5] M. Tanaka, E. Saitoh, H. Miyajima, T. Yamaoka and Y. Iye, Phys. Rev. B **73** 052411 (2006).
[6] R. F. Wang *et al.*, Nature **439**, 303 (2006).
[7] N. Rougemaille *et al.*, Phys. Rev. Lett. **106**, 057209 (2011).
[8] S. Zhang *et al.*, Nature **500**, 553-557 (2013).
[9] B. Canals *et al.*, Nature Commun. **7**, 11446 (2016).
[10] G.-W. Chern, M. J. Morrison and C. Nisoli, Phys. Rev. Lett. **111**, 177201 (2013).
[11] I. Gilbert *et al.*, Nature Phys. **10**, 671 (2014).
[12] I.-A. Chioar *et al.*, Phys. Rev. B **90**, 220407R (2014).
[13] I.-A. Chioar *et al.*, Phys. Rev. B **90**, 064411 (2014).
[14] F. Montaigne *et al.*, Sci. Rep. **4**, 5702 (2014).
[15] J. Drisko, S. Daunheimer and J. Cumings, Phys. Rev. B **91**, 224406 (2015).
[16] I.-A. Chioar, N. Rougemaille and B. Canals, Phys. Rev. B **93**, 214410 (2016).
[17] J. Hamp, R. Moessner and C. Castelnovo, Phys. Rev. B **98**, 144439 (2018).
[18] Y. Perrin, B. Canals and N. Rougemaille, Nature **540**, 410-415 (2016).
[19] O. Sendetskyi *et al.*, Phys. Rev. B **93**, 224413 (2016).
[20] E. Östman *et al.*, Nature Phys. **14**, 375-379 (2018).
[21] A. Farhan *et al.*, Sci. Adv. **5,** eaav6380 (2019).
[22] M. J. P. Gingras, Spin ice in *Highly Frustrated Magnetism*, edited by C. Lacroix, P. Mendels, and F. Mila (Springer, New York, 2009).
[23] C. L. Henley, Ann. Rev. Condens. Matter Phys. **1**, 179 (2010).
[24] S. T. Bramwell, M. J. P. Gingras and P. C. W. Holdsworth, Spin ice in *Frustrated Spin Systems*, edited by H. T. Diep (World Scientific, 2013).
[25] M. E. Brooks-Bartlett, S. T. Banks, L. D. C. Jaubert, A. Harman-Clarke and P. C. W. Holdsworth, Phys. Rev. X **4**, 011007 (2014).
[26] S. Petit *et al.*, Nature Phys. **12**, 746-750 (2016).
[27] E. Lefrancois *et al.*, Nature Commun. **8**, 209 (2017).
[28] G. Möller and R. Moessner, Phys. Rev. B **80**, 140409(R) (2009).
[29] G.-W. Chern, P. Mellado and O. Tchernyshyov, Phys. Rev. Lett. **106**, 207202 (2011).
[30] This dynamical freezing is a consequence of the large energy barriers separating quasidegenerate ice configurations, which prevent the system from finding more energetically favorable states. Because of these energy barriers, going from one low-energy configuration to another one having a lower (or the very same) energy requires to excite transient high-energy states, which become statistically unlikely as the temperature is reduced. Single spin-flips are then less and less probable as the dipolar kagome ice approaches the SL1/SL2 phase transition: the single spin-flip dynamics freezes. See R. G. Melko and M. J. P. Gingras, J. Phys.: Condens. Matter **16**, R1277 (2004).
[31] S. A. Daunheimer, O. Petrova, O. Tchernyshyov and J. Cumings, Phys. Rev. Lett. **107**, 167201 (2011).
[32] K. K. Kohli *et al.*, Phys. Rev. B **84**, 180412(R) (2011).
[33] Z. Budrikis *et al.*, Phys. Rev. Lett. **109**, 037203 (2012).
[34] J. P. Morgan, A. Stein, S. Langridge and C.H. Marrows, Nat. Phys. **7**, 75 (2011).
[35] Z. Budrikis, P. Politi and R. L. Stamps, New J. Phys. **14**, 045008 (2012).
[36] A. Farhan *et al.*, Phys. Rev. Lett. **111**, 057204 (2013).
[37] V. Kapaklis *et al.*, Nat. Nanotechnol. **9**, 514 (2014).
[38] A. Farhan *et al.*, Phys. Rev. B **96**, 064409 (2017).
[39] S. Zhang *et al.*, Phys. Rev. Lett. **109**, 087201 (2012).
[40] L. Anghinolfi *et al.*, Nature Commun. **6**, 8278 (2015).
[41] N. Rougemaille *et al.*, New J. Phys. **15**, 035026 (2013).
[42] S. Gliga *et al.*, Phys. Rev. Lett. **110**, 117205 (2013).
[43] Y. Perrin, B. Canals and N. Rougemaille, Phys. Rev. B **99**, 224434 (2019).
[44] V. D. Nguyen, Y. Perrin, S. Le Denmat, B. Canals and N. Rougemaille, Phys. Rev. B **96**, 014402 (2017).
[45] G. W. Paterson *et al.*, Phys. Rev. B **100**, 174410 (2019).
[46] See Supplemental Material [url] for the choice of the simulation parameters, which includes Ref. 47.
[47] A. Vansteenkiste *et al.* AIP Advances **4**, 107133 (2014).
[48] In a conventional artificial square lattice, type I and type II vertices are two times and four times degenerate, respectively [6]. The energy gap between those vertex types originates from the anisotropic nature of the dipolar interaction and from the different distances between the four magnets constituting a vertex. In our modified kagome ice, the notch lifts the sixfold degeneracy of the vertex and leads to two energy levels having a degeneracy two (type 1) and four (type 2) [in blue and red in Fig. 2(a)]. But here the energy gap has a micromagnetic origin, as the nanomagnets are connected at the vertex sites.
[49] J. C. Gartside *et al.*, Nature Nanotech. **13**, 53

(2018).
[50] See Supplemental Material [url] for details on the Monte Carlo simulations, which includes Refs. [51–54].
[51] I. Syozi, Prog. Theor. Phys. **6**, 306-308 (1951).
[52] K. Kano and S. Naya, Prog. Theor. Phys. **10**, 158-172 (1953).
[53] R. Moessner, Phys. Rev. B **57**, R5587-R5589 (1998).
[54] A. S. Wills, R. Ballou and C. Lacroix Phys. Rev. B **66**, 144407 (2002).